Paper No.
11622

NACE INTERNATIONAL CORROSION 2018 Conference & Expo

Effectiveness of an imidazoline-type inhibitor against CO_2 corrosion of mild steel at elevated temperatures (120°C-150°C)

Yuan Ding, Bruce Brown, David Young, Marc Singer
Institute for Corrosion and Multiphase Technology
Department of Chemical & Biomolecular Engineering
Ohio University
342 West State Street
Athens, OH 45701

Abstract

Production of oil and gas from increasingly aggressive geologic environments requires the development of appropriate corrosion mitigation strategies, including the selection of corrosion inhibitors with adequate performance characteristics. In this study, the inhibition performance of a diethylenetriamine tall oil fatty acid imidazoline-type inhibitor (DETA/TOFA imidazoline) against CO_2 corrosion of an API 5L X65 carbon steel was studied at two temperatures, 120°C and 150°C. The corrosion measurements were performed in a CO_2 saturated 1 wt.% NaCl electrolyte, *via* electrochemical measurements, in a standard autoclave and in a specially designed two-autoclave system. A two-autoclave design was developed and adopted for transferring heated, deoxygenated aqueous electrolyte to the autoclave containing the working electrode, thereby limiting specimen exposure to oxygen and eliminating long transition times associated with solution heating/cooling. At 120°C, the two autoclave setup successfully enabled the identification of the true corrosion inhibitor behavior by preventing build-up of corrosion product layers. At this temperature, the imidazoline type inhibitor did adsorb on the steel surface with an inhibition efficiency of 61%. At 150°C, the presence of inhibitor did not affect the corrosion profile, whatever the autoclave system used. The surfaces of the specimens retrieved from experiments were characterized using scanning electron microscopy (SEM), energy-dispersive X-ray spectroscopy (EDS) and X-ray diffraction (XRD). At 150°C, the rapid formation of Fe_3O_4, rather than the effect of inhibitor, seemed to have controlled the corrosion behavior. However, the presence of the imidazoline-type inhibitor impeded the formation of corrosion product layers.

Key words: High temperature, CO_2 corrosion, corrosion inhibition, imidazoline-type inhibitor, magnetite

Introduction and Objectives

Depletion of hydrocarbon reservoirs in relatively shallow strata has driven the oil and gas industry to drill deeper in order to access hitherto untapped resources[1]. Due to geologic reasons[2], these new reservoirs usually feature high temperature and high pressure characteristics. This can present acute technical challenges for the industry, one of which being the management of high temperature CO_2 corrosion of tubing material. Many mitigation methods have been developed and applied to address this challenge. The most cost-effective technique, used widely in transmission pipelines as well as downhole, involves injection of corrosion inhibitors.

Generally, corrosion inhibitors mitigate corrosion predictably and effectively at lower temperatures (up to 80°C). The efficiency and cost effectiveness of corrosion inhibitors have driven operators and researchers to attempt to extend their domain of validity to higher temperatures(100°C-180°C)[3–5]. Efforts have been made to develop specific inhibitor formulations that are effective at high temperature[3–5], however, little attention is typically paid to understand the underlying mechanisms behind failed or successful inhibition.

In an earlier research described by the authors of this paper, inhibition performance and adsorption characteristics of an imidazoline-type inhibitor were investigated up to 80°C[6]. Inhibition performance decreased with temperature, suggesting that desorption from the steel surface was favored at higher temperature. However, whether the same adsorption/desorption behavior governs the performance of corrosion inhibitor at elevated temperatures (100°C and above) remained unknown.

At higher temperature, CO_2 corrosion product formation has greater complexity. The kinetics for formation of corrosion products is naturally, and significantly, accelerated. In addition, at even higher temperatures (150°C and above) Fe_3O_4 can also form[6, 7] in addition to $FeCO_3$. Possible interactions between this corrosion product and inhibitor molecules are unknown.

Experimental evaluation of corrosion inhibitors at high temperature also brings its own sets of challenges. Autoclaves are typically used in this environment, but the limited volume of the systems (usually under 10 liters) and the inherent difficulty to monitor and control electrolyte chemistry create an environment where aqueous chemistry, in particular pH and $[Fe^{2+}]$, can change and corrosion products can be formed rapidly. Consequently, design of new experimental setups that can effectively minimize experimental artifacts is of paramount importance.

In the present study, the effect of an imidazoline-type inhibitor on the corrosion behavior of carbon steel was investigated at 120°C and 150°C in two different autoclave systems:

- The first autoclave system consisted of a standard “closed system” autoclave equipped with an inhibitor injector. The experiment protocols necessitated

lengthy heating (and cooling) periods where steel specimens were immersed in the electrolyte and corrosion products could form, even before injection of inhibitors.

- The second autoclave system included two autoclaves connected to each other, one of them used to heat (and cool) the electrolyte and the other used to perform the inhibition test. In this scenario, the steel specimens and solution were heated separately. The heating (and cooling) periods were eliminated as the specimens were exposed to the inhibited solution at the tested conditions only. This limited the formation of corrosion product compared to the one autoclave system.

In addition, the role of the thermal stability of the corrosion inhibitor was also investigated to understand its effect on its performance at high temperature.

Corrosion rates were measured using linear polarization resistance (LPR). The surfaces of the specimens retrieved after the experiments were characterized using scanning electron microscopy (SEM), energy-dispersive X-ray spectroscopy (EDS) and X-ray diffraction (XRD).

Experimental Procedure

Equipment

Single autoclave system

The single autoclave system contains a 4-liter autoclave equipped with an inhibitor injector, as shown in Figure 1(a). There are three electrodes mounted through the autoclave's stainless steel lid, namely an Ag/AgCl reference probe, a Pt-coated Nb counter electrode, and the working electrode (API 5L X65 steel, UNS K03014, Table 1). In addition, the pH is monitored using a ZrO_2-based pH probe that can operate in high temperature and high pressure environments; calibration is performed using standard solutions. Linear polarization resistance (LPR) and open circuit potential (OCP) measurements are performed using a Gamry† Reference 600™ potentiostat. The temperature in the autoclave is continuously monitored and controlled using a digital reader. The test electrolyte is stirred using an impeller.

In the injection system, 200 mL of 1 wt.% NaCl containing the desired molar amount of corrosion inhibitor is loaded into a pressure bomb; the electrolyte is purged beforehand with N_2 to minimize the presence of O_2. The injection bomb is connected to the autoclave lid by appropriate fittings. When it is the time for injection, the bomb is pressurized with N_2 so its internal pressure is higher than in the autoclave. Upon opening of the valve connecting the bomb and the autoclave, the pressure difference drives the inhibitor solution into the autoclave.

† Trade Name.

Each experiment was conducted in 3L of 1 wt.% NaCl solution. After it was poured into the autoclave body, the electrolyte was purged continuously with CO_2 for more than 2 hours at 80°C to remove O_2. After purging, the stainless steel lid, with pre-installed specimens, electrodes and probes, was attached to the autoclave body. The gas outlet and inlet valves were then closed and the temperature set to the desired target value. When the desired temperature was achieved, the system was pressurized with CO_2 to apply an additional 2 bar of pressure. Electrochemical measurements (LPR and OCP) were started after this pressurizing step, for use as a baseline condition. After completion of the baseline measurements, the inhibitor solution was injected into the system. The corrosion rate was monitored using LPR for 24 hours. Measurements were carried out every 30 minutes over the first 2 hours and every hour for the next 22 hours. Bulk solution pH was measured at the end of the experiments and solution samples were taken for Fe^{2+} concentration analysis. The system was then cooled to around 80°C, depressurized, the lid detached, and the hanging specimens removed. The retrieved specimens were stored in a N_2 flushed cabinet for subsequent surface characterization by SEM and EDS. The corrosion product was characterized using XRD. Solution samples were taken immediately after the injection of corrosion inhibitor and at the end of the experiment for analysis by ultraviolet-visible (UV-Vis) spectroscopy.

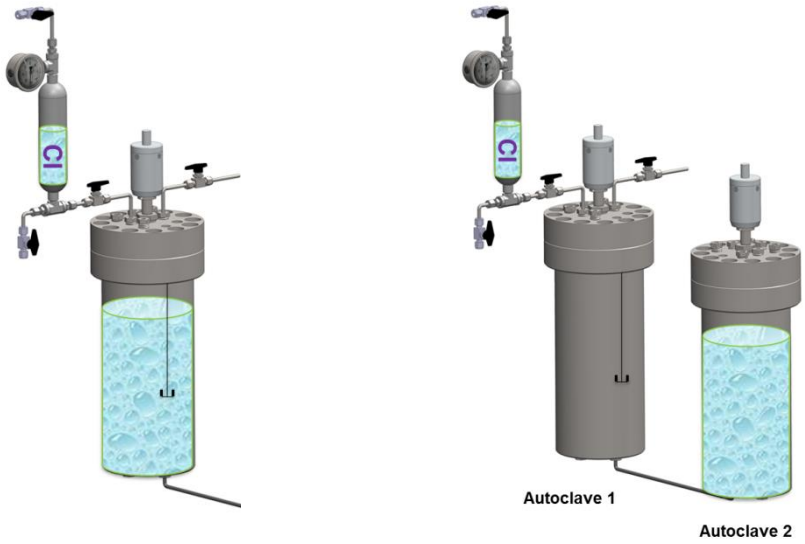

(a) Single autoclave system **(b) Two-autoclave system**

Figure 1. Configuration of the autoclave systems (CI stands for solution containing inhibitor)

Table 1. Chemical composition of API 5L X65

C	Mn	Si	S	P	V	Mo	Ni	Fe
0.13%	1.16%	0.26%	0.009%	0.009%	0.047%	0.16%	0.36%	Balance

The test conditions are given in Table 2. The critical micelle concentration (CMC) of the imidazoline-type inhibitor used in the set of experiments was measured as 36ppm (by volume) at 25°C. However, in the earlier work[6], 1 CMC of the inhibitor was proven to be insufficient to control corrosion at higher temperatures (50-80°C). Therefore, in this work, the system was "overdosed" with 440ppm corrosion inhibitor at the tested temperatures.

Table 2. Test matrix at 120°C and 150°C

Parameters	Description
Temperature/°C	120, 150
Imidazoline-type inhibitor concentration/ppm	0, 440
Solution	3L 1 wt.% NaCl saturated with CO_2
Initial pH at 80°C	4.30
Material	APL 5L X65
Impeller speed/rpm	200
Electrochemical measurements	LPR, OCP

Two-autoclave system

The second autoclave system is shown in Figure 1(b). The major difference between the single autoclave system and the 2-autoclave system is that the solutions and the specimens are heated to the desired temperature in two different autoclaves. Otherwise, the components in the autoclave are similar. There are also three electrodes as well as a high temperature high pressure pH probe mounted through the autoclave lid. The temperature is monitored and controlled using the same digital controller. The solution is mixed with an impeller set to 200rpm.

The procedure in the two-autoclave system is slightly different from the single-autoclave system. The main differences are in the heating up and cooling down periods. First, the solution was heated at 80°C in autoclave 2 and sparged with CO_2 continuously to remove oxygen. Autoclave 1, which contained the specimens but no electrolyte, was also sparged with CO_2 and heated to 80°C. After 2-3 hours of purging, both autoclaves were closed and heated to the desired temperature. Later, the solution was transferred from autoclave 2 to autoclave 1 with N_2 gas by opening valves between the two autoclaves. After the solution was completely transferred, electrochemical measurements were started in autoclave 1. One LPR measurement was taken as a baseline and then the inhibitor solution was injected into the system through the injection vessel. Similarly, the corrosion rate was monitored using LPR for 24 hours. Bulk solution pH was measured at the end of the experiments and solution samples were taken for Fe^{2+} concentration analysis. After electrochemical measurements ended, autoclave 1 was pressurized with N_2 and the valve between the two autoclaves was opened. The pressure difference drove the solution from autoclave 1 back into autoclave 2. Therefore, the cooling-down of solution and specimens were also done in

two separate autoclaves. Autoclave 1 was then cooled to around 80°C, depressurized, the lid detached, and the hanging specimens removed following the same procedure as in the single-autoclave system. The retrieved specimens were characterized by SEM, EDS and XRD. Solution samples were also taken immediately after the injection of corrosion inhibitor and at the end of the experiment for analysis by UV-Vis spectroscopy.

The new "two-autoclave" system yields the following improvements compared to the traditional "single-autoclave":

- The solution was heated in a separate autoclave. This significantly limited any potential ingress of oxygen. The measured oxygen level at the end of purging was below 3ppb.
- By heating the solutions and the specimens in two separate autoclaves, the heating period decreased from 3-4 hours to less than 20 minutes. This substantially limited the formation of corrosion product.
- The solutions and the specimens were cooled down separately as well. The cooling-down period was reduced from 5-6 hours to 2-3 hours. By keeping the specimens in inert conditions (N_2 environment) at the end of experiments, the nature of the corrosion products was not altered during the cooling period.

The tested conditions, which are the same in both autoclave systems, are given in Table 2.

Results and Discussion

Corrosion behavior of X65 steel at 120°C with and without inhibitor in the single autoclave system

The changes of LPR corrosion rates with time for tests conducted with 440ppm imidazoline-type inhibitor and without inhibitor are shown in Figure 2.

In the absence of inhibitor, the corrosion rate initially increased to around 10 $mm \cdot y^{-1}$ and remained at that value for about 8 hours, before gradually dropping to 1 $mm \cdot y^{-1}$ over the next 16 hours. This indicates that in the first several hours of the test, the formation of a $FeCO_3$ layer was not favored and that the corrosion rate was mainly "bare steel" corrosion governed by the partial pressure of CO_2. However, as corrosion progressed, water chemistry changed in the autoclave's closed system (increase in pH and $[Fe^{2+}]$) and resulted in development of local environments favoring the growth of iron carbonate on the working electrode surface. This led to formation of an increasingly protective corrosion product layer and a decrease in the corrosion rate. The presence of iron carbide in the steel microstructure may have also accelerated this phenomenon by acting as an additional mass transfer barrier.

The test performed with corrosion inhibitor shows a different behavior. After the inhibitor was injected into the system, the corrosion rate immediately dropped and stabilized at around 3 $mm \cdot y^{-1}$ over a period of about 3 hours. This behavior is similar to that previously observed at temperatures of 25°C to 80°C in the authors' earlier work[6]. This

demonstrates that the inhibitor can still reduce corrosion significantly at 120°C. However, the corrosion rate at the end of the experiment was still high. It is noteworthy that, at the conclusion of each test, the uninhibited and inhibited corrosion rates were very close but it is postulated that this behavior was obtained for two very different reasons, specifically formation of corrosion product layer for the uninhibited test and presence of inhibitor for the inhibited test; this is discussed in more detail below. However, the main purpose of this study is not to investigate the effect of corrosion product layers or the interaction between corrosion product layers and chemical inhibition. Consequently, the true effect of chemical inhibition could be masked in this test as a consequence of using a single “closed system” autoclave.

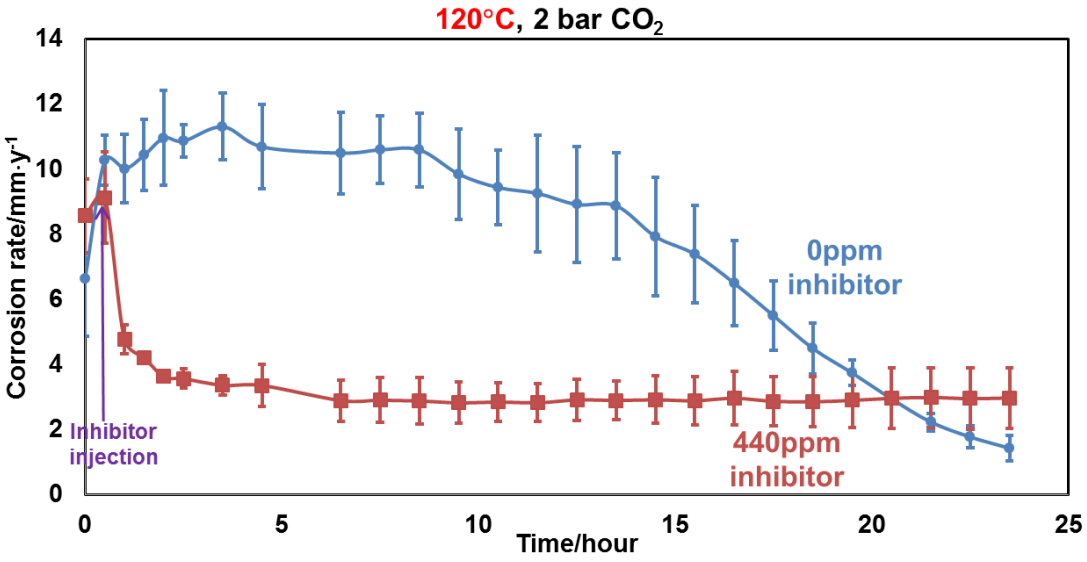

Figure 2. Corrosion rate with/without corrosion inhibitor at 120°C and pCO_2 2 bar in the single autoclave system (B=23mV/decade)

In order to confirm that the development of an iron carbonate layer was the reason behind the decrease in corrosion rate in the uninhibited test, specimen surfaces were characterized using SEM and EDS. The SEM images and EDS data are shown in Figure 3 (a) and (b) for the uninhibited and inhibited tests, respectively.

Although all surfaces show extensive signs of corrosion, distinctive features were still observed. The surfaces of specimens retrieved in the absence of corrosion inhibitor showed two morphological features, one crystallized with an oblong growth habit (zone 1 of Figure 3(a)) and the other flat (zone 2 of Figure 3 (a)). However, for specimens retrieved after exposure to 440 ppm imidazoline-type inhibitor, the surface appeared relatively flat as aligned rods (zone 1 of Figure 3 (b)) or possess plate-like features (zone 2 of Figure 3 (b)).

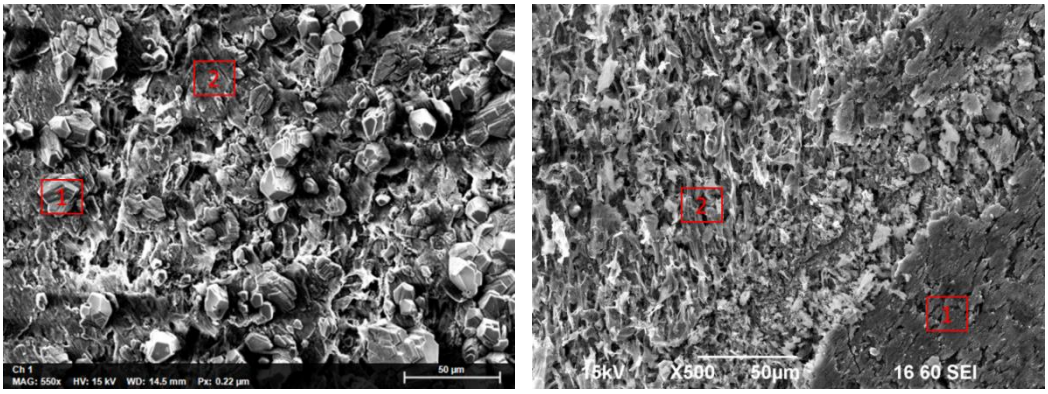

(a) 0 ppm inhibitor **(b)440 ppm inhibitor**

Figure 3. SEM images of the steel surfaces after 120°C test

XRD patterns of the specimens exposed to the corrosive environments at 120°C are shown in Figure 4. The main corrosion product was iron carbonate for the tests without corrosion inhibitor (Figure 4 (a)). However, no iron carbonate peak was observed in the specimens obtained in the inhibited test (Figure 4 (b)).

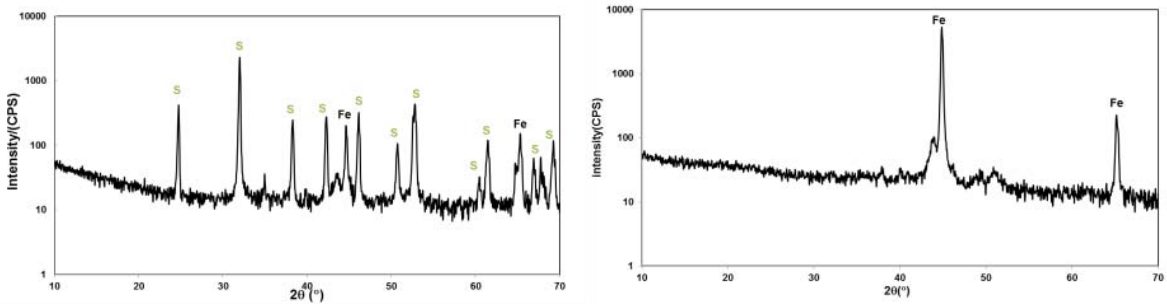

(a) 0ppm inhibitor **(b) 440ppm inhibitor**

Figure 4.XRD patterns of the specimens retrieved after experiments in the single autoclave system at 120°C (S stands for iron carbonate, and Fe stands for iron).

Cross-section images and EDS data are shown in Figure 5. The SEM images show that there was a corrosion product layer on the steel surface in experiments conducted in the absence of corrosion inhibitor. Combined with the XRD results, it can be concluded that the layer is an iron carbonate layer. In contrast, the corrosion product on the surface of the inhibited specimen did not display any coherent structure comparable to what was observed for the uninhibited test. The missing iron carbonate peaks suggest that its formation was suppressed with the presence of corrosion inhibitor. Instead, the layer visible on top of the steel surface in Figure 5 (b) is postulated to be iron carbide.

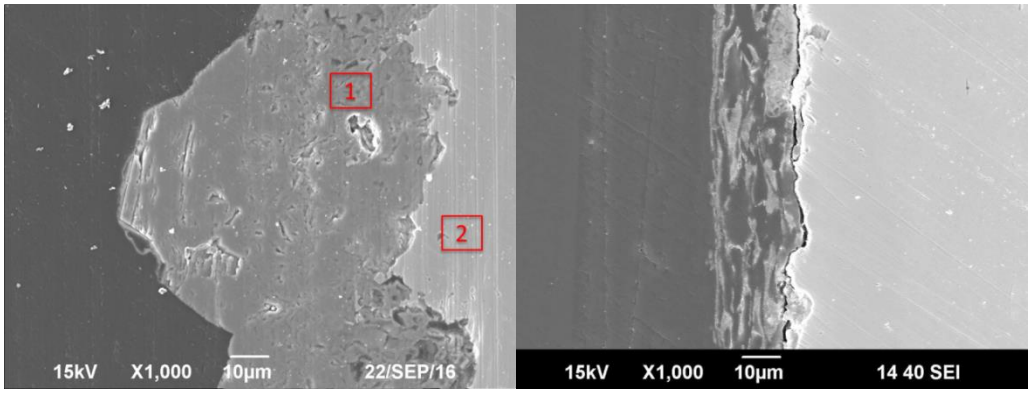

(a) 0 ppm inhibitor **(b) 440 ppm inhibitor**

Figure 5. SEM images and EDS analysis of steel cross-sections of specimens retrieved from tests conducted at 120°C (from left to right: epoxy→corrosion product layer→steel matrix).

Corrosion behavior of X65 steel at 150°C with and without corrosion inhibitor in the single autoclave system

Corrosion rates of API 5L X65 specimens exposed to different concentrations of corrosion inhibitor at 150°C are shown in Figure 6. With 0 ppm corrosion inhibitor, the corrosion rate initially increased then dropped and stabilized at around 1 $mm \cdot y^{-1}$; as for the previous test performed as 120°C, this is likely due to the formation of a corrosion product layer. With 440 ppm corrosion inhibitor, the corrosion rate decreased steadily over the testing period until it reached a stable value of around 2 $mm \cdot y^{-1}$. Since the results with 0 and 440 ppm of inhibitor seem very close, an additional experiment with 880 ppm corrosion inhibitor was carried out. However, the corrosion behavior with 880ppm of inhibitor also ended up very similar to that observed for the other two tests. This is significantly different from what was observed at 120°C, which showed a sharp decrease in inhibited corrosion rate immediately after injection and not a gradual decrease as seen at 150°C. At this point, it is unclear what, if any, effect the presence of corrosion inhibitor had on the corrosion behavior.

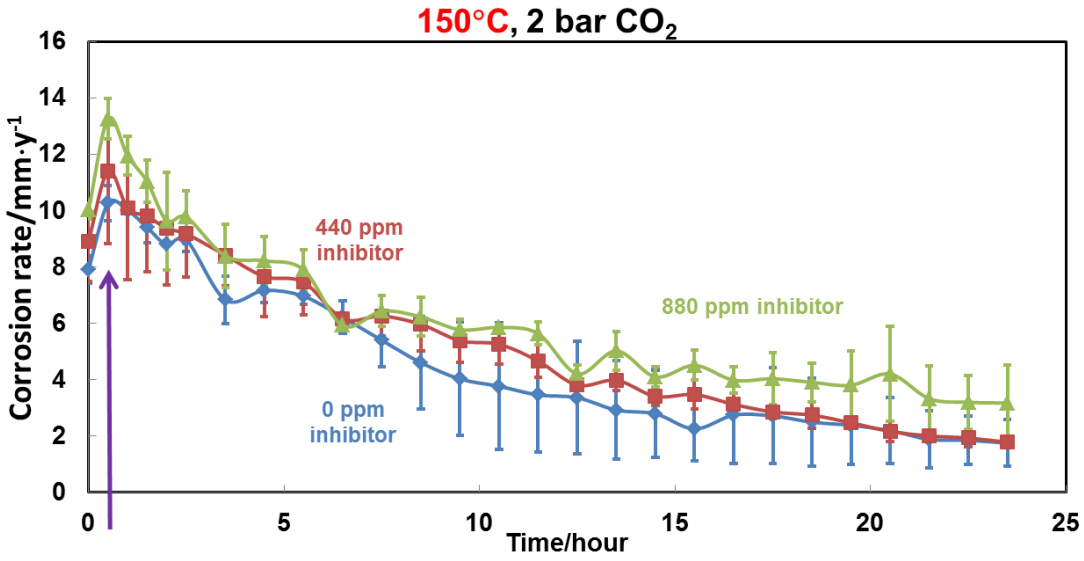

Figure 6. Corrosion rate for different concentrations of corrosion inhibitor at 150°C (B=23mV/decade). Purple arrow line shows when inhibitor was injected.

The surface of the specimen was characterized by SEM, as shown in Figure 7 (a), (b), and (c). The surface morphologies of the steel specimen with and without corrosion inhibitor show clear differences. Without corrosion inhibitor, the surface seems relatively uniform and the presence of a homogeneous corrosion product layer is evident. However, in the presence of corrosion inhibitor (440 or 880 ppm), a porous, heterogeneous layer is present on the metal surface which is postulated to be iron carbide.

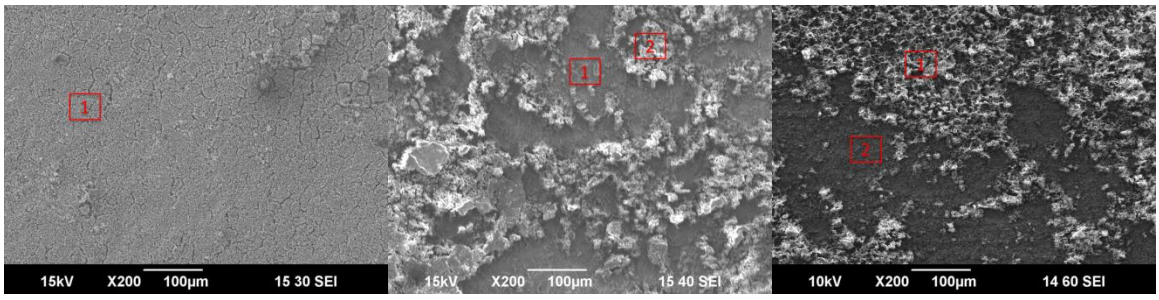

(a) 0ppm inhibitor **(b) 440ppm inhibitor** **(c) 880ppm inhibitor**

Figure 7. SEM of X65 steel surface with various concentrations of corrosion inhibitor at 150°C

The XRD patterns of the specimens retrieved from the experiments at 150°C in the single autoclave system are shown in Figure 8. At 150°C, a new type of corrosion product, Fe_3O_4, was observed for the experiments at 150°C, even in the absence of inhibitor. This was also observed in other researchers' work[7, 8]. It is noticeable that in the tests with corrosion inhibitor, the XRD patterns feature low intensity peaks of Fe_3O_4 and high intensity peaks of iron. Conversely, the XRD pattern associated with the

uninhibited specimen shows high intensity peaks for Fe_3O_4, which suggests that the thickness of the Fe_3O_4 layer for the test with corrosion inhibitor was thinner than for the test without corrosion inhibitor.

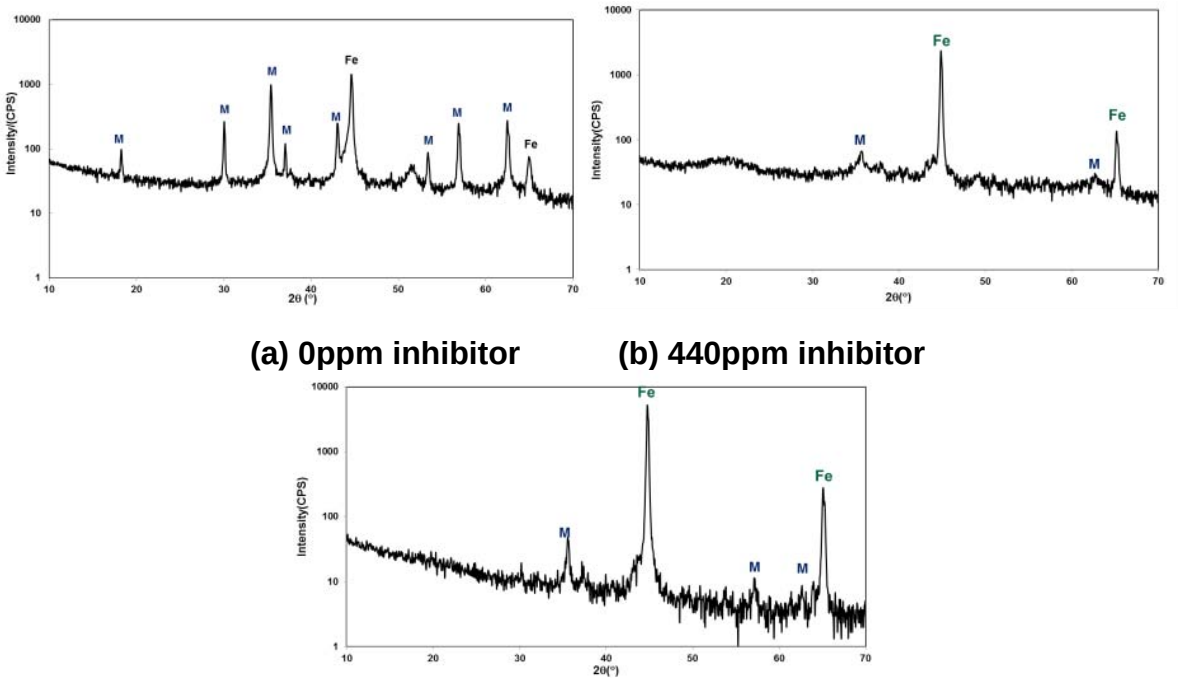

(a) 0ppm inhibitor **(b) 440ppm inhibitor**

(c) 880ppm inhibitor

Figure 8. XRD patterns of the specimens retrieved after experiments in the single autoclave system at 150°C (S stands for iron carbonate, M for Fe_3O_4 and Fe for iron).

In addition, specimen cross-sections were examined by SEM/EDS as shown in Figure 9 (a), (b), and (c). Figure 9 (a) clearly indicates the presence of a thick corrosion product layer (40μm) for the uninhibited conditions. However, no apparent layer was observed in inhibited environments, as shown in Figure 9 (b), or (c). This again confirms that the formation of corrosion product was significantly hindered by the presence of the imidazoline-type corrosion inhibitor.

Although the experiments performed at 120 and 150°C yielded interesting results, the use of a single autoclave system could have significantly altered the data and masked the true effect of the inhibitor. As stated earlier, the main issue with the single autoclave system was the long heating and cooling transition periods that could have led to the formation of corrosion product even before the inhibitor was injected. To address this issue, the two-autoclave system was developed so that the solution and the specimens were heated separately in order to reduce the transition period and, hence, the formation of corrosion product thereby isolating the effect of corrosion inhibitor.

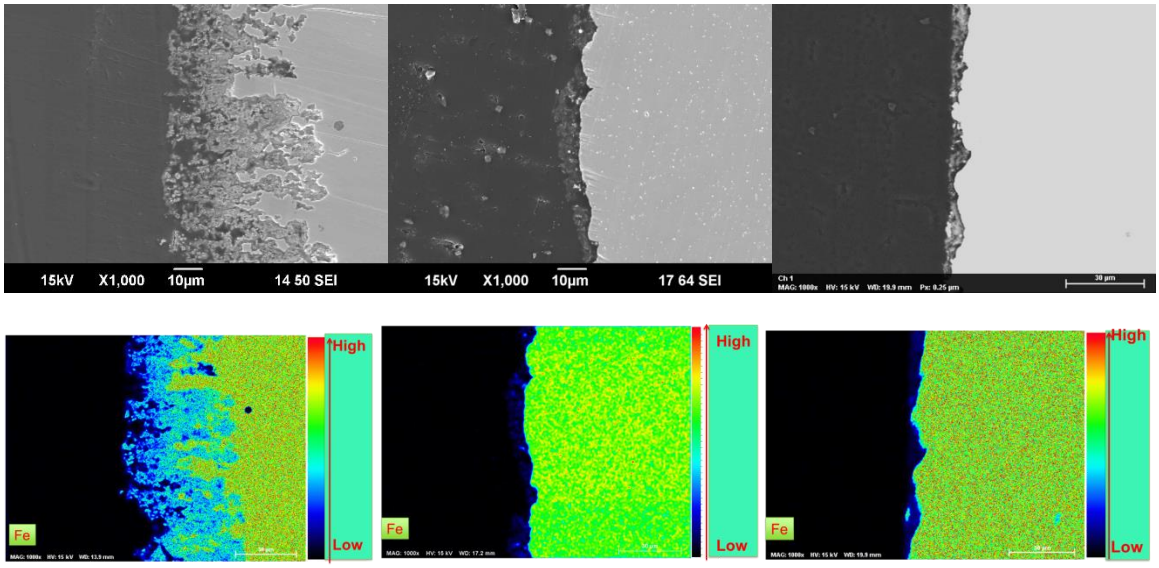

(a) 0 ppm inhibitor **(b) 440 ppm inhibitor** **(c) 880 ppm inhibitor**

Figure 9 Cross-sections images and EDS Fe element mapping of specimens with various concentrations of corrosion inhibitor at 150°C

Corrosion behavior at 120°C in the two-autoclave system

The change in LPR corrosion rates with time with and without imidazoline-type inhibitor is shown in Figure 10. In the uninhibited system, the corrosion rate was initially around 5 $mm{\cdot}y^{-1}$ and increased gradually to 9 $mm{\cdot}y^{-1}$ during the first 1 hour. After that, corrosion rate remained around 9 $mm{\cdot}y^{-1}$ for the next 22 hours of exposure. The stable corrosion rate suggests that the formation of corrosion product layers was prevented in the 24 hour experiment without corrosion inhibitor. This behavior indicates that the formation of corrosion product is at least significantly delayed in the new system and likely due to a decrease in the carbon steel specimen exposure time to the solution.

In the inhibited system (440 ppm of inhibitor), the corrosion rate dropped quickly from an initial corrosion rate of 7 $mm{\cdot}y^{-1}$ to 3.5 $mm{\cdot}y^{-1}$ after the addition of corrosion inhibitor. The corrosion rate then remained stable for the rest of the experiment. This behavior is similar to what was previously observed at 120°C in the 1 autoclave system. The similar value of the inhibited corrosion rate suggests that the performance of the inhibitor is correctly captured in both autoclave systems.

Since the uninhibited corrosion rate could be determined with more confidence in the two-autoclave system, the inhibition efficiency of the imidazoline-type inhibitor could then be calculated as:

$$Inhibition\ efficiency = \left(1 - \frac{inhibited\ corrosion\ rate}{uninhibited\ corrosion\ rate}\right) \times 100\% = 61\% \quad (1)$$

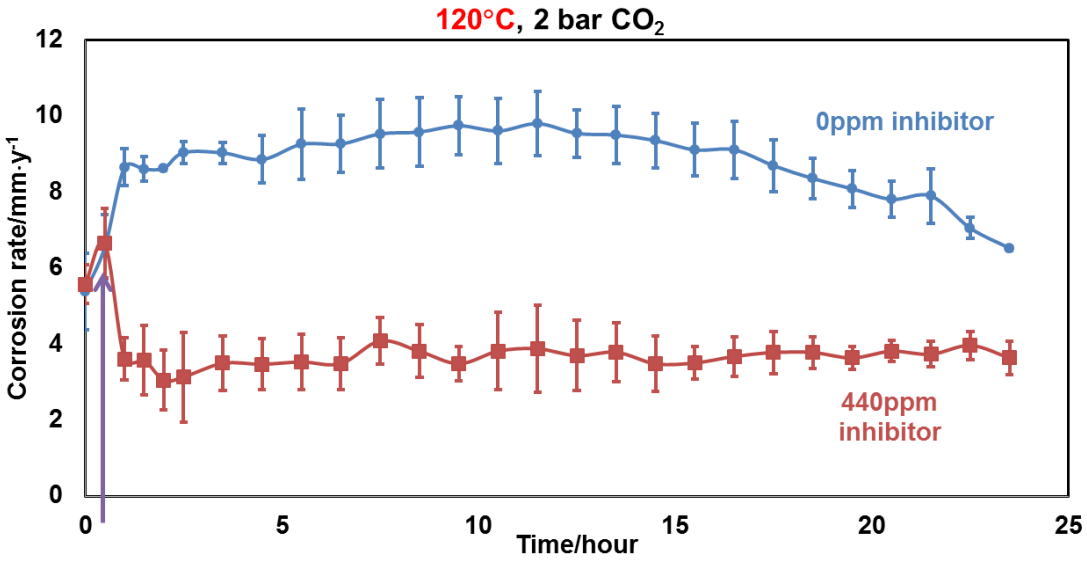

Figure 10. Corrosion rate with/without corrosion inhibitor at 120°C and 2 bar pCO_2 in the two-autoclave system (B=23mV/decade).

In the absence of inhibitor, the fact that the corrosion rate remained constant during the entire duration of the test suggests that no protective corrosion product layer formed. This is different from what was observed in the single autoclave system. To confirm the absence of an iron carbonate layer, the surface was characterized using XRD, SEM and EDS.

The XRD patterns of the specimens recovered for the "120°C" experiment in the new system are shown in Figure 11. The major difference from the single autoclave system is that even without corrosion inhibitor, the $FeCO_3$ peaks are absent. This is likely because, in the new system, the heating period was completely by-passed. This decreases the exposure time of the steel specimen to the electrolyte and minimizes the buildup of Fe^{2+} in solution; this delayed the formation of iron carbonate.

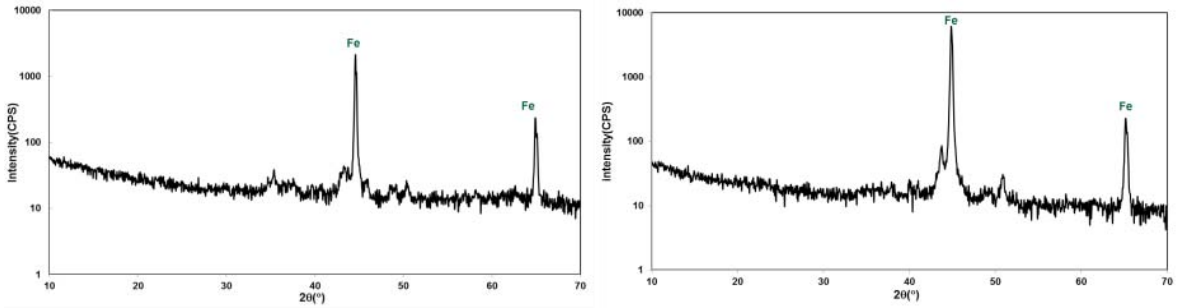

(a) 0ppm inhibitor (b) 440ppm inhibitor

Figure 11 XRD patterns of the specimens retrieved after experiments in the two autoclave system at 120°C (Fe stands for iron).

Figure 12 demonstrates formation of a very porous corrosion product layer. The absence of $FeCO_3$ crystals is also noticeable. In Figure 12 (b), the surface appears relatively flat with sheet-like features, often associated with iron carbide, partly covering the surface. The formation of $FeCO_3$ was clearly delayed at 120°C in the new system.

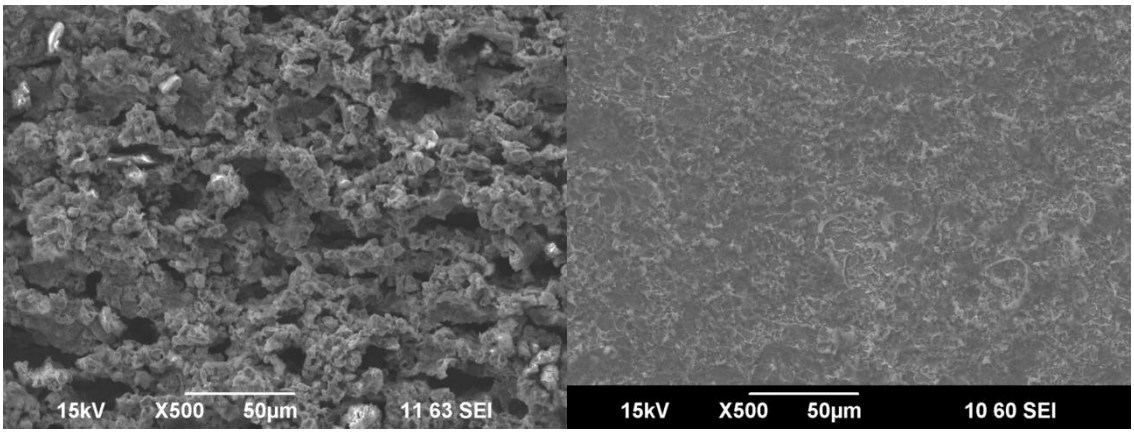

(a) 0 ppm inhibitor **(b) 440 ppm inhibitor**

Figure 12. SEM images of specimen surfaces from 120°C experiments

Corrosion behavior in the 2-autoclave system with and without corrosion inhibitor at 150°C

Corrosion rates of mild steel specimens exposed to different concentrations of the imidazoline-type corrosion inhibitor at 150°C are shown in Figure 13. At 0 ppm corrosion inhibitor, the corrosion rate increased slightly at the beginning of the test and then decreased gradually. Once again, the decrease of the corrosion rate was likely due to the formation of corrosion products. With 440 ppm corrosion inhibitor, the corrosion rate trend was again very similar to what was observed without corrosion inhibitor. The corrosion rate decreased to around 3 $mm \cdot y^{-1}$ after the 24 hours experiment. Similarly, with 880 ppm inhibitor added into the system, the corrosion rate also monotonously decreased to around 6 $mm \cdot y^{-1}$. These results are very similar to what was obtained in the single autoclave system. This suggests that the addition of corrosion inhibitor did not inhibit the corrosion rate at 150°C.

The XRD patterns of the specimens recovered from this set of experiments are shown in Figure 14. The patterns are similar to the XRD data in the single autoclave system at 150°C (Figure 8). In the absence of corrosion inhibitor, the Fe_3O_4 peak intensity is high, which suggests that a thick layer of magnetite formed on the surface of the specimen. In the presence of inhibitor, the same Fe_3O_4 peak was detected but at a much lower intensity.

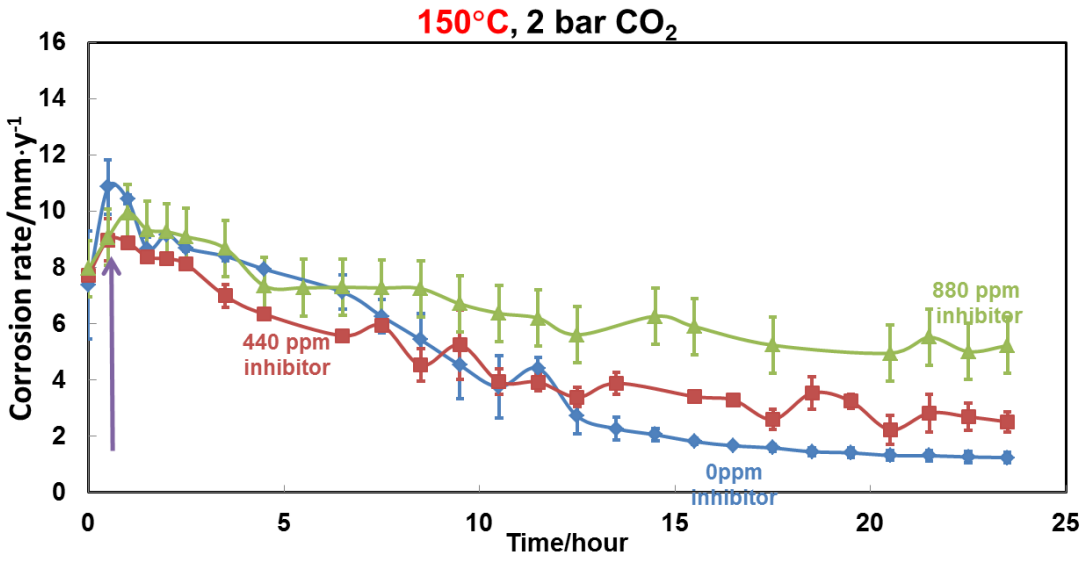

Figure 13. Corrosion rates with various amount inhibitors at 150°C in the two autoclave system. (2 bar pCO_2)

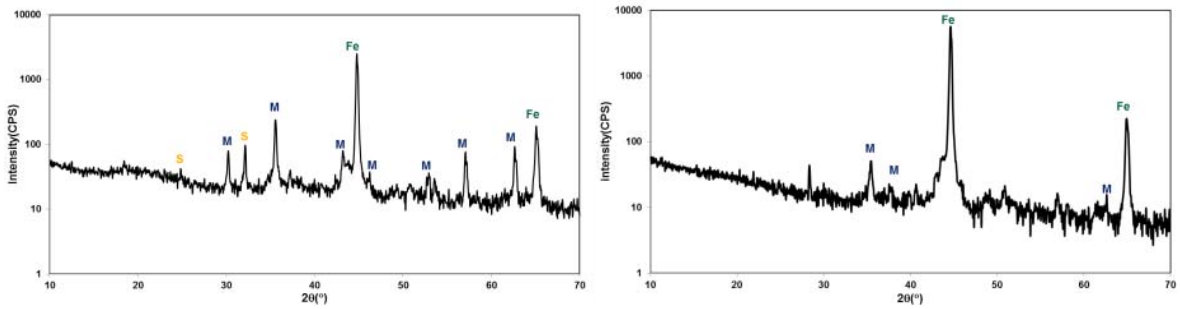

(a) 0ppm inhibitor **(b) 440ppm inhibitor**

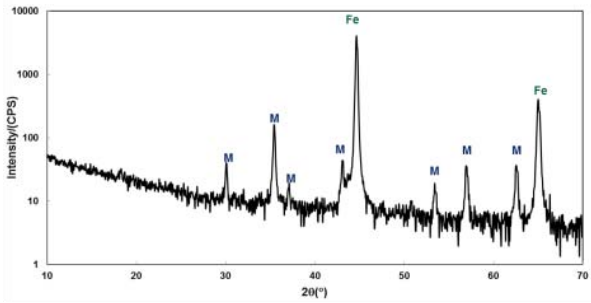

(c) 880ppm inhibitor

Figure 14. XRD patterns of the specimens retrieved after experiments in the two-autoclave system at 150°C. (Fe stands for iron, S stands for $FeCO_3$ and M stands for Fe_3O_4)

The surface morphologies of the specimens, considering the tests with and without corrosion inhibitor, are shown in Figure 15 (a), (b), (c). They are distinctly different. In

uninhibited environments, the surface of the mild steel specimen featured a uniform surface with crystallized structures on top. However, the surfaces of the specimen collected from the inhibited tests were uneven and partly covered with porous layers.

The cross-section images of the corrosion product layers obtained through tests with and without corrosion inhibitor are shown in Figure 16 (a), (b), (c). In the uninhibited system (Figure 16 (a)), a corrosion product layer was observed with a thickness of 30-40 μm. However, in the inhibited system, no obvious layer was identified. This is analogous to what was observed in the single autoclave system (Figure 8).

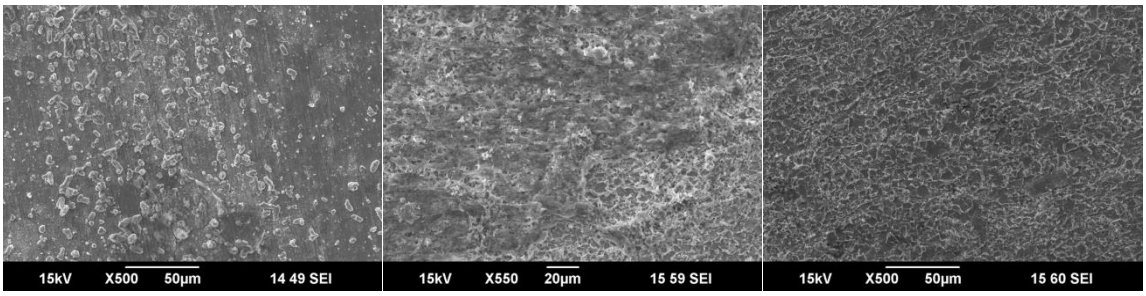

(a) 0 ppm inhibitor (b) 440 ppm inhibitor (c) 880 ppm inhibitor

Figure 15. Surface morphology of X65 steel for various concentrations of corrosion inhibitor at 150°C

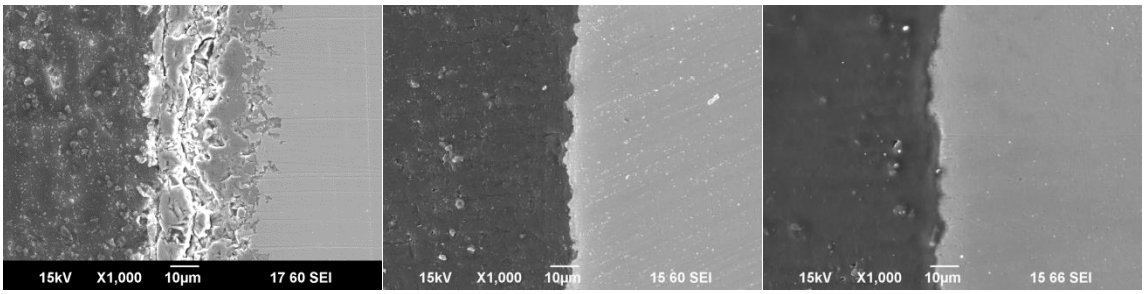

(a) 0 ppm inhibitor (b) 440 ppm inhibitor (c) 880 ppm inhibitor

Figure 16. Cross-section images of the mild steel specimens for various concentrations of corrosion inhibitor at 150°C (epoxy on the left and steel substrate on the right side of each image)

Discussion of the interaction between of corrosion product and imidazoline-type inhibitor

The development of the two-autoclave setup and associated procedures helped minimize the effect of experimental artifacts relating to long heating and cooling periods and the build-up of Fe^{2+} in solution before the actual test was started. Because of the new design, the steel specimens were only exposed to a short period of pre-corrosion before inhibitor injection. In addition, the specimens were cooled down in an inert environment to avoid modification of the specimen surface layer. These changes in

setup and procedures clearly affected the 120°C uninhibited test results for which the formation of iron carbonate was delayed, enabling the specimen to corrode uniformly during the entire duration of the test. However, no noticeable changes in the uninhibited results of the 150°C experiment were observed, whether the test was performed in the single or two autoclave setups. This suggests different uninhibited corrosion mechanisms for these two tested temperatures, which are most likely due to the type corrosion products that formed on the steel surface. Yet, at 150°C, the inhibited experimental results remained relatively unaffected by the change in test setup.

To better understand the role of different corrosion product, the types of corrosion product encountered in the two-autoclave system are summarized in

Table 3.

Table 3. Corrosion products in various environments

Temperature/°C	XRD patterns of products without inhibitor	XRD patterns of products with inhibitor
120	None found	None found
150	$FeCO_3$/Fe_3O_4	Fe_3O_4

Compared to the single-autoclave system, the formation of $FeCO_3$ was delayed at 120°C in an uninhibited system. However, at 150°C, the formation of Fe_3O_4 was not significantly affected. In addition, the formation of corrosion products was impeded by the presence of corrosion inhibitor at both temperatures. The corrosion product formation on the inhibition effect of the imidazoline-type inhibitor is also evident by combining the results from cross-section examination and the XRD patterns. The cross-section images clearly show that there seems to be no formation of corrosion product layers. Although XRD confirms the presence of Fe_3O_4 at 150°C, a thick layer was only seen in the absence of corrosion inhibitor.

In addition, the water chemistry at the end of each experiment in the single-autoclave system was recorded and is given in Table 4. The water chemistry in the two-autoclave system is similar to what was observed in the single autoclave system and, hence, is not discussed further here. The bulk iron carbonate saturation and scaling tendency in the table were calculated based on an in-house CO_2 corrosion model. In all the tested conditions, the corrosion product should have formed rapidly since the systems were highly supersaturated with $FeCO_3$. However, corrosion product layers were only observed in uninhibited conditions. This again confirms that the imidazoline-type inhibitor played a role in inhibition of corrosion product formation.

By inspecting the types of corrosion products in the different environments tested, it seems that the formation of Fe_3O_4 governs the corrosion mechanism at 150°C and that its formation occurs rapidly at the beginning of each experiment. No matter what autoclave system was used, Fe_3O_4 was always observed at 150°C in the XRD patterns.

Literature also shows that the formation of Fe_3O_4 at higher temperatures is fast[9, 10]. In addition, Fe_3O_4 has a protective role against corrosion. In this study, the experimental corrosion rates indeed quickly decreased due to the rapid formation of Fe_3O_4. In the absence of inhibitor, the Fe_3O_4 grew very thick, providing additional mass transfer limitation, which might also contribute to the low final corrosion rate at the end of the test. Comparatively, the fact that inhibitor could impede the formation of additional Fe_3O_4, as shown in Figure 9 and Figure 16, could be the reason behind the slightly higher final corrosion rates (Figure 13).

Table 4. Water chemistry at the end of each experiment in the single-autoclave system

Test conditions	C(Fe^{2+})/ppm	pH	Bulk $FeCO_3$ saturation	Scaling tendency at the steel surface
120°C, 0ppm	121	5.90	167	20
120°C, 440ppm	107	5.80	144	11
150°C, 0ppm	129	5.87	195	75
150°C, 440ppm	80	5.80	165	34
150°C, 880ppm	113	5.93	225	86

The role of thermal stability of the corrosion inhibitor

The imidazoline-type inhibitor is reported to be unstable at higher temperatures and to hydrolyze into its amide precursor[11, 12]. The degradation of corrosion inhibitor might also affect the corrosion inhibition. A method using UV-Vis was developed to measure the imidazoline-type inhibitor concentration in 1 wt.% NaCl solution[13].

The inhibitor concentration at the beginning and the end of each experiment was measured and recorded as shown in Table 5. The residual inhibitor percentage was defined as:

$$Residual\ inhibitor\ percentage = \frac{Inhibitor\ concentration}{Initial\ inhibitor\ concentration} \quad (2)$$

The residual percentage was found to be similar in the two-autoclave system, at around 50-60%. There was clearly a loss of the active component (imidazoline-type) of the corrosion inhibitor at higher temperatures.

Table 5. Imidazoline-type inhibitor concentration in the single autoclave system

Test conditions	Initial concentration/ppm	Final concentration/ppm	Residual inhibitor percentage/%
120°C, 440ppm	257	127	49
150°C, 440ppm	309	194	63
150°C, 880ppm	614	295	48

Some black oily residue was found on the autoclave wall after the experiments. This residue was insoluble in water, so UV-Vis spectroscopy was not readily able to identify this species. Therefore, Fourier transform infrared (FTIR) spectroscopy was used to identify components of the oily residue. The spectrum is shown in Figure 17. Two peaks associated with the imidazoline are observed. Peak 1 at around 1645 cm^{-1} and peak 2 at 1556 cm^{-1} stand for the stretch (st) mode of the C=O bond and the stretch and symmetric (st sy) mode of N-C=O bond[14], respectively, which only exist in the amide. It is worthy to mention that in the literature[11], for a imidazoline-type inhibitor, there is a peak at 1610 cm^{-1} which represents the stretch mode of C=N. However, this peak was not observed in the spectrum. Therefore, it can be concluded the oily residue likely consisted of amide precursor only.

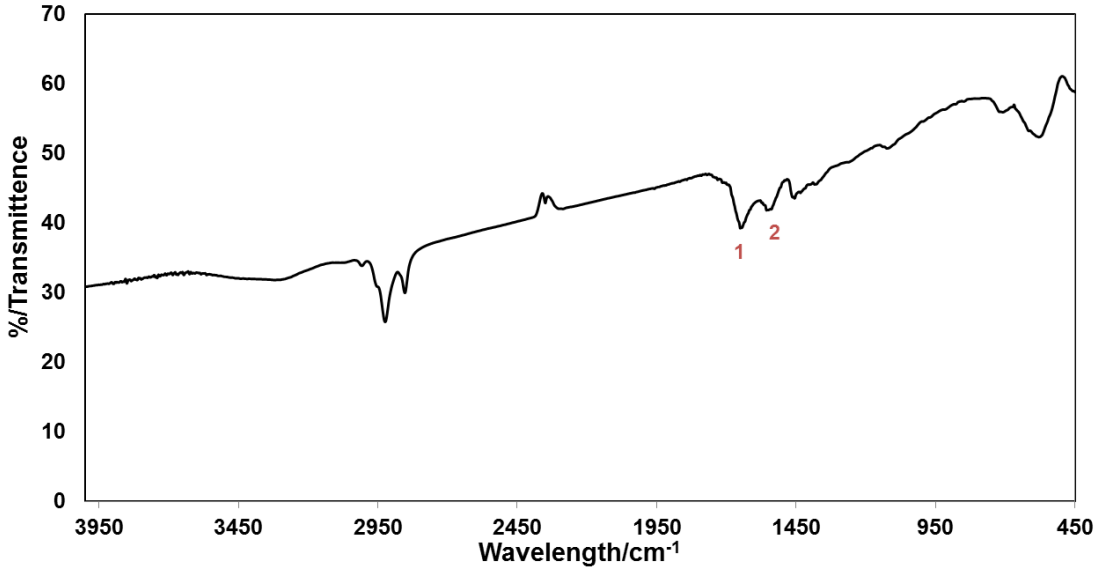

Figure 17. FTIR spectrum of black gum retrieved from experiment (peak 1: C=O st, peak 2: N-C=O, st sy)

From the above results, it can be concluded that the imidazoline-type inhibitor was partially hydrolyzed into its amide precursor at high temperature. Due to its low solubility in water, the amide accumulated on the wall of the autoclave. About 40-50% of the imidazoline inhibitor was lost this way due to thermal degradation. However, there was still plenty of “intact” imidazoline inhibitor left in the system. This means that the failure

of the inhibition at higher temperatures (150°C) was not entirely due to the degradation of imidazoline-type inhibitor.

Conclusions

Mild steel corrosion inhibition tests were performed at 120 and 150°C in a CO_2 environment with an imidazoline-type inhibitor (diethylenetriamine tall oil fatty acid imidazoline (DETA/TOFA imidazoline)). The experiments were performed in a standard autoclave and in a specially designed two-autoclave system. The two-autoclave design was developed to limit specimen exposure to oxygen and eliminating long transition times associated with solution heating/cooling.

In a single-autoclave system, the uninhibited corrosion results seem to be affected by the formation of corrosion product ($FeCO_3$ at 120°C and Fe_3O_4 at 150°C), possibly due to the long heating transition period. This, in turn, masked the true role of the imidazoline-type inhibitor on the corrosion process.

Using the two-autoclave system, the formation of iron carbonate in the uninhibited test was mostly avoided at 120°C. The efficiency of the inhibitor could then be clearly determined at 61%. At 150°C, the rapid formation of Fe_3O_4 could not be prevented and seemed to control the corrosion behavior with or without inhibitor. At this temperature, the presence of inhibitor had no visible effect on the corrosion rate.

The imidazoline-type inhibitor also showed scale inhibiting abilities. With the presence of corrosion inhibitor, there was no noticeable corrosion product layer on the steel surface at 120°C or 150°C (except for a very thin Fe_3O_4 layer detected in the XRD patterns at 150°C).

The imidazoline-type inhibitor degraded into its amide precursor at tested temperatures. However, only about 40% to 50% of the inhibitor was lost due to the hydrolysis of imidazoline. Consequently, the failure of inhibition at 150°C was not entirely due to the degradation of imidazoline-type inhibitor.

Acknowledgements

The author would like to thank the following companies for their financial support:

Anadarko, Baker Hughes, BP, Chevron, CNOOC, ConocoPhillips, DNV GL, ExxonMobil, M-I SWACO (Schlumberger), Multi-Chem (Halliburton), Occidental Oil Company, PTT, Saudi Aramco, Shell Global Solutions, SINOPEC (China Petroleum), TOTAL, and Wood Group Kenny.

References

1. R. W. Bentley, “Global oil & gas depletion: an overview,” *Energy Policy* 30 (2003): pp. 189-205.

2. A. Shadravan and M. Amani, “HPHT 101-What petroleum engineers and geoscientists should know about high pressure high temperature wells environment,” *Energy Science and Technology* 4.2 (2012): pp.36-60.

3. N. U. Obeyesekere, A. R. Naraghi, L. Chen, S. Zhou, and S. Wang, “Novel corrosion inhibitors for high temperature applications,” CORROSION 2005, paper no. 05636.

4. S. Ramachandran, Y. S. Ahn, M. Greaves, V. Jovancicevic, and J. Bassett, “Development of high temperature high pressure corrosion inhibitor,” CORROSION 2006, paper no. 06377.

5. A. Palencsár, E. Gulbrandsen, and K. Kosorú, “High temperature testing of corrosion inhibitor performance,” CORROSION 2013, paper no. 2610.

6. Y. Ding, B. Brown, D. Young, S. Nesic, and M. Singer, “Effect of temperature on adsorption behavior and corrosion inhibition performance of imidazoline-type inhibitor,” CORROSION 2017, paper no. 9350.

7. T. Tanupabrungsun, D. Young, B. Brown, and S. Nešić, “Construction and verification of pourbaix diagrams for CO_2 corrosion of mild steel valid up to 250° C,” CORROSION 2012, paper no. 0001418.

8. T. Tanupabrungsun, B. Brown, and S. Nesic, “Effect of pH on CO_2 corrosion of mild steel at elevated temperatures,” CORROSION 2013, paper no. 2348.

9. J. E. Castle and H. G. Masterson, “The role of diffusion in the oxidation of mild steel in high temperature aqueous solutions,” *Corrosion Science* 6.3-4, (1966): pp. 93-96.

10. J. Robertson, “The mechanism of high temperature aqueous corrosion of steel,” Corrosion Science, 29. 11-12, (1989): 1275-1291.

11. J. A. Martin and F. W. Valone, “The existence of imidazoline corrosion inhibitors,” *Corrosion*, 41.5 (1985): pp. 281-287.

12. V. Jovancicevic, S. Ramachandran, and P. Prince, “Inhibition of carbon dioxide corrosion of mild steel by imidazolines and their precursors,” *Corrosion*, 55.5 (1999): pp. 449-455.

13. NACE student poster session. “Determination of imidazoline-type inhibitor concentrations by UV-Vis spectroscopy,” CORROSION 2017.

14. E. Pretsch, P. Bühlmann, C. Affolter, *Structure determination of organic compounds*, 4th ed. (Springer Berlin Heidelberg, 2009), pp. 293-295.